Mechanical validation of viscoelastic parameters for different interface pressures using the Kelvin-Voigt fractional derivative model

Aldo Tecse[1], Stefano E. Romero[1], Carlos Romero,[2] Roozbeh Naemi[3] and Benjamin Castaneda[1]

***Abstract*— The knowledge of the biomechanical properties of tissues is useful for different applications such as disease diagnosis and treatment monitoring. Reverberant Shear Wave Elastography is an approach that has reduced the restrictions on wave generation to characterize the shear wave velocity over a range of frequencies. This approach is based on the generation of a reverberant field that is generated by the reflections of waves from inhomogeneities and tissue boundaries that exist in the tissue. The Kelvin-Voigt Fractional Derivative model is commonly used to characterize elasticity and viscosity of soft tissue when using shear wave ultrasound elatography. These viscoelastic characteristics can be then validated using mechanical test such as stress relaxation. During RSWE acquisition, the effect of interface pressure, induced by pushing the probe on the skin through the gelpad, on the viscous and elastic characteristics of tissue can be investigated. However the effect of interface pressure on the validity viscous and elastic characteristics was not investigated. Therefore, the purpose of this study is to contrast the estimation of the viscoelastic parameters at different thickness of gelpad with mechanical measurements. The experiments were conducted in a tissue-mimicking phantom. The results confirm that the relaxed elastic constant (μ_0) can be depreciated. In addition, a higher congruence was found in the viscous parameter (η_α) estimated at 6 and 7 mm. On the other hand, a difference in the order of fractional derivative (α) was found.**

***Keywords*— Elastography, Stress relaxation, Shear Waves, Reverberant fields, Ultrasound.**

I. INTRODUCTION

Biomechanical properties of tissues constitute necessary knowledge for different medical applications such as modeling, disease diagnosis and treatment monitoring.

Particularly, Ultrasound (US) is an imaging modality of interest because of its low-cost in contrast with MRI or OCT. After 30 years of the first images of local elasticity properties on soft tissues, multiple approaches have been developed. Among the US elastography techniques, Reverberant Shear Wave elastography (RSWE) have gained attention for its potential for clinical applications in multiple tissues such as breast [1]–[3], liver [1]–[3], eye [4], [5], and plantar tissue [6], [7]. This technique produces quantitative results and uses external vibration forces, thus it has a deeper penetration than other techniques such as Acoustic Radiation Force Impulse (ARFI) or Transient Elastography. Also, pressure waves generated by the transducer, for example with ARFI, can generate thermal artifacts which reduces the quality of estimation [8], [9]. Inhomogeneities and organ boundaries inside the body usually produce reflections of the pressure waves produced by the external forces [10]. Techniques such as ARFI and Crawling waves elastography apply directional filters to reduce the impact of the reflections [1], [11]. The application of filters might produce the loss of information. In contrast, RSWE is based on the formation of a reverberant field (RF), hence it is benefited by the natural reflections. RSWE register the shear wave speed (SWS) inside the reverberant field, assuming it is assumed that a distribution of shear waves exists, oriented across all directions in 3D and continuous in time [2]. Finally, for a perfectly elastic, isotropic and incompressible material, the SWS (c_s) is related to its corresponding Young's modulus: $E = 3\rho c_s^2$. Where ρ is the density of the material (assumed to be $1000\ \mathrm{kg/cm^3}$ for soft tissues) and c_s is the SWS [12].

The effect of interface pressure (IP), induced by pushing the probe on the skin through the gelpad, on the SWS was previously assessed using US-RSWE [6]. However, the effect of the IP on the viscous and elastic characteristics of tissue has not yet been investigated. The aim of this study is to contrast the viscous and elastic parameters characterized in the time and frequency domain using RSWE and MM information, respectively. We perform the inverse problem analysis, the viscoelastic parameters for Kelvin-Voigt Fractional Derivative (KVFD) and Maxwell were estimated using the least-square regression. The experiments were performed on a tissue-mimmicking phantom. Three mechanical sources were used to generate vibration at five excitation frequencies. Then, the SWS was estimated by recovering the particle velocity with an ultrasound transducer. Finally, a phantom core was extracted to perform Mechanical Measurments (MM) of Stress Relaxation.

II. THEORY

A. Reverberant Shear Wave Elastography

A reverberant field can be simulated under the hypothesis of a diffuse field by the superposition of multiple plane waves in all the directions in a certain point ε and at a time t [4], [13].

$$\hat{P}(t,\varepsilon) = \sum_q \hat{P}_q \cdot e^{j(k_s \boldsymbol{n}_q \cdot \varepsilon - \omega t)} \tag{1}$$

*The authors acknowledge the support of CONCYTEC (Peru). In particular, Stefano Romero was under the doctoral scholarship program in Computer Science (174-2020-FONDECYT-PUCP).

[1]Aldo Tecse, Stefano E. Romero, and Benjamin Castaneda are with the Department of Engineering, Pontificia Universidad Católica del Perú, Lima, Peru a.tecse@pucp.edu.pe, sromerog@pucp.pe, castaneda.b@pucp.edu.pe

[2]Carlos Romero is with the Laboratorio de materiales cj.romero@pucp.pe

[3]Roozbeh Naemi is with the School of Health, Science and Wellbeing, Staffordshire University, Staffordshire, UK r.naemi@staffs.ac.uk

Where q represents each direction, $\boldsymbol{n}_q$ represents each one of the unit vectors uniformly distributed in 4π steradians. The resultant velocity of these plane waves is represented by (1)

$$V(t,\varepsilon) = \sum_q \boldsymbol{n}_q \hat{v}_q \cdot e^{j(k_s \boldsymbol{n}_q \cdot \varepsilon - \omega t)} \tag{2}$$

Considering $\hat{v}_q$ through the relation of acoustic impedance of plane waves:

$$\hat{v}_q = \frac{n_q \hat{P}_q}{\rho C} \tag{3}$$

Where ρ is the medium density and C is the sound speed inside the medium.

B. Shear Wave Speed estimation

If the particle velocity in (2) is measured along the z-axis, then $V_z(\epsilon,t) = \boldsymbol{V}(\epsilon,t)\cdot\widehat{e_z}$, where $\widehat{e_z}$ is a unit vector in the z direction, see Fig. 1. Given the reverberant field, closed form complex analytical solutions can be found for the spatial auto-correlation of such fields along parallel and orthogonal directions to the measurement axis $\widehat{e_z}$. In the orthogonal case, the auto-correlation of the reverberant field along the lateral axis is given by:

$$B_{V_z V_z}(\Delta\varepsilon_x) = \frac{\beta}{2}\left[j_0(k\Delta\varepsilon_x) - \frac{j_1(k\Delta\varepsilon_x)}{k\Delta\varepsilon_z}\right] \tag{4}$$

where β is the expected value of squared particle velocity magnitude v_{ql}^2 over both q and l realizations; j_0 and j_1 are spherical Bessel functions of the first kind of zero and first order, respectively; and $\Delta\epsilon_x = \Delta\epsilon \cdot \widehat{e_x}$ with $\widehat{e_x}$ as a unit vector along the x-axis. On the other hand, for the parallel case, the spatial auto-correlation of the reverberant field is taken along the z-axis:

$$B_{V_z V_z}(\Delta\varepsilon_z) = \frac{\beta}{2}\left[\frac{j_1(k\Delta\varepsilon_z)}{k\Delta\varepsilon_z}\right] \tag{5}$$

From (5) and (6), we can notice that a Curve Fitting (CF) can be applied in a region of a reverberant field in order to estimate the local parameter $k_e st$. Hence, we can find the SWS by $c_s = \omega/k_e st$ [4].

C. KVFD Models

Several viscoelastic models have been proposed to describe the viscous and elastic behavior of soft tissue [14]. One of the most common viscoelastic models is the KVFD model, see Fig. 1. For this study, the frequency-dependent SWS was used to optimize the parameters associated with KVFD model through (6).

$$\mathrm{SWS}_{\mathrm{KVFD}}(f_v) = \sqrt{\frac{\mu_0 + \eta_\alpha \cos\left(\frac{\pi\alpha}{2}\right)(2\pi f_v)^\alpha}{3\rho}} \tag{6}$$

where μ_0 represents the relaxed elastic constant, η_α the viscoelastic parameter, α the order of the fractional derivative and f_v the frequency.

Kelvin-Voigt Fractional Derivative (KVFD)

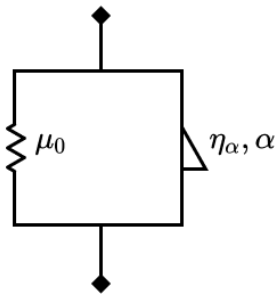

Fig. 1. Viscoelastic models used for this study

Besides, MM of stress relaxation tests were used to characterize the viscoelastic behavior. When a viscoelastic material is held at constant strain, the stress decreases with time. To develop a form of the relaxation function, the applied strain is modeled as a ramp of duration T_0, followed by a hold period of constant strain ε_0 [15]. Therefore, its Laplace transform is given by (8)

$$\varepsilon(s) = \frac{\varepsilon_0}{s^2 T_0}\left(1 - e^{-sT_0}\right) \tag{7}$$

where s is the Laplace domain variable. The constitutive equations of the KVFD model correspond to (9) and (10)

$$\sigma(s) = \mu_0 \varepsilon(s) + \mu_\alpha s^\alpha \varepsilon(s) \tag{8}$$

Hence, replacing $\varepsilon(s)$ in (9) and (10) and applying the inverse Laplace transform, the theoretical response of the stress relaxation response is obtained for the KVFD model in (11) and (12), respectively.

$$\sigma_{\mathrm{KVFD}}(t) = \mu_0 \tfrac{\varepsilon_0}{T_0}\left(tu(t) - (t-T_0)\,u(t-T_0)\right) \quad + \quad \mu_\alpha \tfrac{\varepsilon_0}{\Gamma(2-\alpha)T_0}\left(t^{1-\alpha}u(t) - (t-T_0)^{1-\alpha}\,u(t-T_0)\right) \tag{9}$$

III. Materials and Methods

A. RSWE Experiments

RSWE was applied to the tissue-mimicking phantom by using two external sources at each foot to generate vibrations at 400, 450, 500, 550 and 600 Hz. Three repetitions were performed. Doppler US data was recorded using the Vantage 64LE ultrasound system with a linear array L11-4v (9 MHz). The shear wave speed (SWS) maps were reconstructed by using a curve-fitting algorithm. The mean values at each frequency were fitted to the KVFD and Maxwell models using (6) and (7), respectively.

The thickness of the gel-pad was controlled by applying different pressure values to the probe using a holder. The holder allowed to produce a perpendicular pressure with respect to the phantom surface. Four gel-pad thicknesses 6-9

mm with 1 mm increment were used and three repetitions were performed at each thickness.

B. Mechanical measurements (MM)

Stress relaxation tests were performed on a cylindrical sample (approximately 38 mm in diameter and 33 mm in length) made with the same mixture used to construct the tissue-mimmicking phantom [15], [16]. A universal mechanical testing machine Z0.50 (Zwick/Roell, Ulm, Germany) with a 10 N load cell was used to test the samples. The compression rate and the strain value were adjusted to 0.5 mm/s and 5%, respectively. The tests lasted approximately 700 s. Then, the stress relaxation data was fitted to the KVFD model using (11).

IV. Results

A. MM and curve fitting results

Fig. 2 shows the result of the stress relaxation test and the curve fitting result using the KVFD model using (9). The coefficient of determination (R^2) obtained is of 0.96.

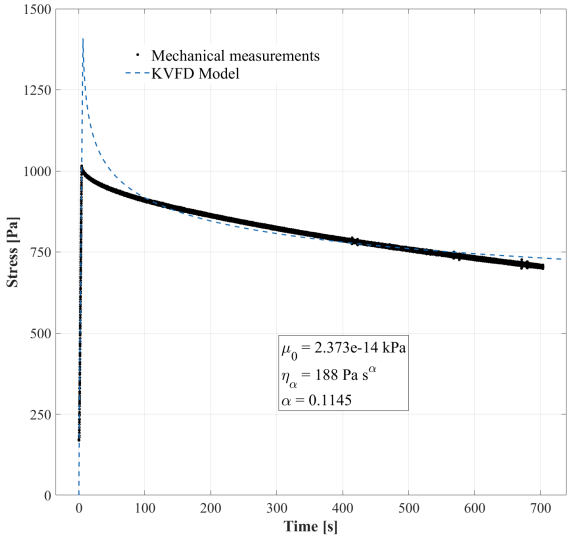

Fig. 2. Fitting of the stress relaxation test with the KVFD model.

B. RSWE and curve fitting results

Fig. 3 shows the SWS-frequency data obtained using US-RSWE for each thickness. Also, the viscous and elastic parameters estimated using the curve fitting algorithm and (6).

V. Discussion

A high value of coefficient of determination was obtained in the curve fitting ($R^2 = 0.96$). Despite this, there is a difference in the peak that occurs before the constant strain is reached. Similar results were reported by [15].

The estimated value for the relaxed elastic constant (μ_0) of the MM is 0 kPa. Similar results were obtained by [1], [15], then the KVFD model reduces to the Spring-Pot model.

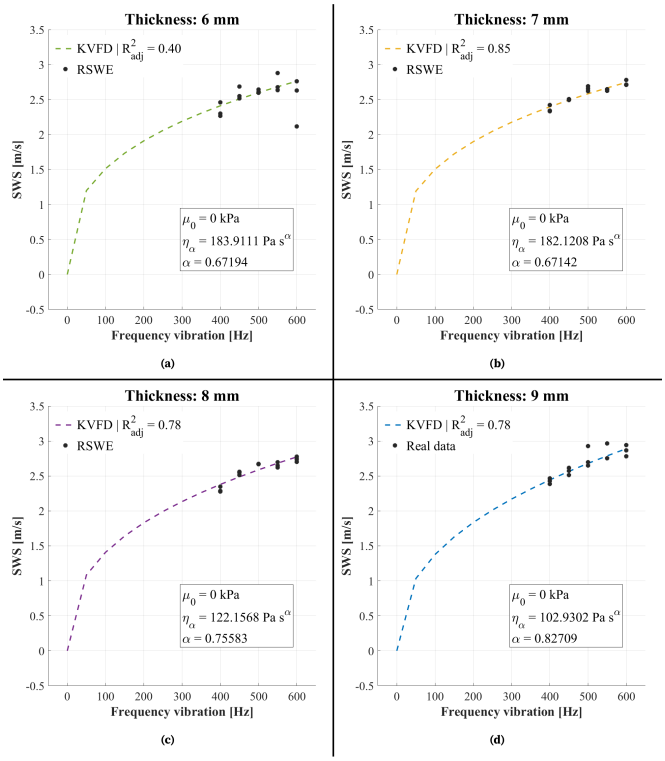

Fig. 3. Fitting of the SWS-frequency data with the KVFD model at a thicknesses of (a) 6 mm, (b) 7 mm, (c) 8 mm, and (d) 9 mm.

Furthermore, the estimated value for the viscous parameter (η_α) of the MM is 180 Pas$^\alpha$. Comparable values were reported for a calibrated phantom [1] using RSWE, but are far away from the values reported by [15] using MM. In contrast, the value of the order of the fractional derivative (α) is close to the values reported by [15] using MM. Then, the order of the fractional derivative (α) that was predicted using either interface pressures cannot estimate the value extracted from the stress relaxation test.

The estimated value for the relaxed elastic constant (μ_0) using MM confirms the value obtained at all gelpad thicknesses. The estimated value for the viscous parameter (η_α) is similar to those estimated by US-RSWE at 6 and 7 mm thicknesses. Also, it can be observed that the value of the viscous parameter (η_α) tends to increase as the thickness of the gel pad is reduced. This is reasonable, since a higher pressure should increase the values of SWS. Furthermore, SWS measurements were consistent at different gel-pad thicknesses with an exception of 6 mm at 600 Hz where relatively low R^2 values (0.47 for KVFD) was observed.

Finally, Fig. 3 shows that a more stable behavior for the SWS-frequency at 7 and 8 mm of thickness. However, the viscous and elastic parameters estimated using MM are closer to the ones estimated at 7 mm. This suggest that a 7 mm thickness for US-RSWE would be ideal for recovering the viscoelastic characteristics.

References

[1] J. Ormachea, B. Castaneda, and K. J. Parker, "Shear wave speed estimation using reverberant shear wave fields: Implementation and feasibility studies," *Ultrasound in medicine & biology*, vol. 44, no. 5, pp. 963–977, 2018.

[2] J. Ormachea, K. J. Parker, and R. G. Barr, "An initial study of complete 2d shear wave dispersion images using a reverberant shear wave field," *Physics in Medicine & Biology*, vol. 64, no. 14, p. 145 009, 2019.

[3] J. Ormachea, R. G. Barr, and K. J. Parker, "2-d shear wave dispersion images using the reverberant shear wave field approach: Application in tissues exhibiting power law response," in *2019 IEEE international ultrasonics symposium (IUS)*, IEEE, 2019, pp. 205–208.

[4] F. Zvietcovich, P. Pongchalee, P. Meemon, J. P. Rolland, and K. J. Parker, "Reverberant 3d optical coherence elastography maps the elasticity of individual corneal layers," *Nature communications*, vol. 10, no. 1, pp. 1–13, 2019.

[5] F. Zvietcovich, A. Nair, M. Singh, S. R. Aglyamov, M. D. Twa, and K. V. Larin, "Dynamic optical coherence elastography of the anterior eye: Understanding the biomechanics of the limbus," *Investigative Ophthalmology & Visual Science*, vol. 61, no. 13, pp. 7–7, 2020.

[6] S. E. Romero, R. Naemi, G. Flores, *et al.*, "Plantar soft tissue characterization using reverberant shear wave elastography: A proof-of-concept study," *Ultrasound in medicine & biology*, vol. 48, no. 1, pp. 35–46, 2022.

[7] R. Naemi, S. E. Romero Gutierrez, D. Allan, *et al.*, "Diabetes status is associated with plantar soft tissue stiffness measured using ultrasound reverberant shear wave elastography approach," *Journal of Diabetes Science and Technology*, p. 1 932 296 820 965 259, 2020.

[8] M. Muller, J.-L. Gennisson, T. Deffieux, M. Tanter, and M. Fink, "Quantitative viscoelasticity mapping of human liver using supersonic shear imaging: Preliminary in vivo feasability study," *Ultrasound in medicine & biology*, vol. 35, no. 2, pp. 219–229, 2009.

[9] C.-Y. Lin, P.-Y. Chen, Y.-W. Shau, and C.-L. Wang, "An artifact in supersonic shear wave elastography," *Ultrasound in medicine & biology*, vol. 43, no. 2, pp. 517–530, 2017.

[10] K. J. Parker, J. Ormachea, F. Zvietcovich, and B. Castaneda, "Reverberant shear wave fields and estimation of tissue properties," *Physics in Medicine & Biology*, vol. 62, no. 3, p. 1046, 2017.

[11] B. Castaneda, L. An, S. Wu, *et al.*, "Prostate cancer detection using crawling wave sonoelastography," in *Medical Imaging 2009: Ultrasonic Imaging and Signal Processing*, International Society for Optics and Photonics, vol. 7265, 2009, p. 726 513.

[12] K. J. Parker, M. M. Doyley, and D. J. Rubens, "Imaging the elastic properties of tissue: The 20 year perspective," *Physics in medicine & biology*, vol. 56, no. 1, R1, 2010.

[13] G. Flores, J. Ormachea, S. E. Romero, F. Zvietcovich, K. J. Parker, and B. Castaneda, "Experimental study to evaluate the generation of reverberant shear wave fields (r-swf) in homogenous media," in *2020 IEEE international ultrasonics symposium (IUS)*, IEEE, 2020, pp. 1–4.

[14] B. Zhou and X. Zhang, "Comparison of five viscoelastic models for estimating viscoelastic parameters using ultrasound shear wave elastography," *Journal of the mechanical behavior of biomedical materials*, vol. 85, pp. 109–116, 2018.

[15] M. Zhang, B. Castaneda, Z. Wu, *et al.*, "Congruence of imaging estimators and mechanical measurements of viscoelastic properties of soft tissues," *Ultrasound in medicine & biology*, vol. 33, no. 10, pp. 1617–1631, 2007.

[16] J. Ormachea, R. J. Lavarello, S. A. McAleavey, K. J. Parker, and B. Castaneda, "Shear wave speed measurements using crawling wave sonoelastography and single tracking location shear wave elasticity imaging for tissue characterization," *IEEE transactions on ultrasonics, ferroelectrics, and frequency control*, vol. 63, no. 9, pp. 1351–1360, 2016.